Modification of Bamboo Fibers/Bio-Based Epoxy Interface by Nano-Reinforced Coatings

Florent Gauvin, Clément Richard, Mathieu Robert
Civil Engineering Department, Carrefour of Innovative Technology and Ecodesign, University of Sherbrooke, Sherbrooke, Quebec, Canada

This study investigates the improvement of the interface between bamboo fibers (BF) and a bio-based epoxy polymer by coating the surface of BF with nanoparticles. Unidirectional BF bundles were dip-coated with three different types of coating: bio-based epoxy, bio-based epoxy containing silanized silica fume, and bio-based epoxy containing starch nanoparticles. Scanning electron microscopy and dynamic contact angle tensiometry were performed to characterize the fiber surface. Tensile tests were conducted to study the benefit of the coating on the fiber properties. Bio-based epoxy/BF composites were molded and both tensile and flexural tests were conducted to study the fiber/matrix interface. Experimental results show that coated BF bundles are more hydrophobic and up to 30% stiffer and resistant than untreated fibers. The nano-reinforced interface enhances the flexural stress and modulus up to 25% and 20%, respectively, depicting a better fiber/matrix interface. **POLYM. COMPOS., 00:000–000, 2016.**

INTRODUCTION

Nowadays, most of the fiber-reinforced polymer (FRP) production is based on synthetic fiber, with mineral or petrochemical origins such as glass, carbon or aramid. In recent years, interest about renewable materials in industry has increased significantly. For instance, natural fibers (NF) have a lot of advantages: they offer a lower density than conventional synthetic fibers and suitable mechanical properties, which make them a potential alternative to glass fiber in FRP [1]. Table 1 depicts properties for E-glass and NF typically used in polymer composites such as flax, hemp, and bamboo [2–5]. The low environmental impact of NF and their biodegradability are required characteristics to create environmental friendliness [6]. Furthermore, the development of NF in FRP stimulates the regional agriculture along the activity of textile industries, allowing to help the decrease of production costs [7]. Tensile strength and Young's modulus of NF are lower than E-glass fiber but their density, such as the one of hemp, coconut, or bamboo, is 2 to 3 times lower.

Bio-sourced and bio-based composites are suitable for many applications. Because of their good mechanical properties and excellent biocompatibility [8], bio-based composites have already been used for many medical applications, such as bone, tooth, and cartilage reparation or implants [8, 9]. In industry, NF-based composites have become more and more popular for applications not facing potential environmental attack, such as interior parts of automotives (interior trims for doors, dashboard, rear shelves, trims, etc.). NF is a complex composite made of cellulose, lignin, and hemicelluloses with porosity called lumens [10, 11].

Among the NF, bamboo is one of the most competitive and suitable fibers for bio-based FRP composite materials: Bamboo fibers (BF) exhibit good mechanical properties [12] for an extremely low density [13]. It is one of the fastest growing plants in the world, an invasive plant, generating huge amount of waste [14]. The use of BF would also reduce the bamboo destruction by combustion, which generates greenhouse effect gases. There are roughly 1,000 species of bamboo worldwide, mostly harvested in Asia [15]. As most of cellulosic fibers, BF are constituted of cellulose, hemicelluloses, and lignin ($>$ 90 weight%) among other constituents such as protein, pectin or ashes ($<$ 10 weight%). Moreover, bamboo structure is unique among NF with an unidirectional arrangement in tissues and the cell wall leading to fully unidirectional fibers, extremely well suited for FRP applications [16]. However, there are some major drawbacks limiting the application of NF. Due to the growing and harvest conditions, NF, and in particular bamboo, have inhomogeneous properties along their surface [17]. Because of their nature, cellulosic fibers are highly hydrophilic and, therefore, have a poor interaction with polymer matrices [18]. This results in the creation of a weak interface between the fibers and the matrices in addition to an uneven dispersion of the fibers [19]. The fiber/matrix interface controls the load transfer between the fiber and the matrix and, therefore, tailors the mechanical properties of the

Correspondence to: M. Robert; e-mail: mathieu.robert2@usherbrooke.ca
DOI 10.1002/pc.24097
Published online in Wiley Online Library (wileyonlinelibrary.com).

TABLE 1. List of conventional synthetic and natural fibers.

Fibers	Young's modulus E (GPa)	Ultimate elongation A (%)	Tensile strength (Mpa)	Density (g/cm^3)
Synthetic fibers				
E-Glass	70–73	3	2000–3500	2.54
Natural fibers				
Flax	12–85	1–4	600–2000	1.53–3.2
Hemp	35	1.6	389–900	1.07
Bamboo	11–32	2.5–3.7	140–800	0.6–1.1

whole composite. The interface also influences the water uptake of the material, which can pave the way for swelling and decrease of the mechanical properties [20]. Furthermore, cellulosic fibers are irreversibly damaged by the hydrolysis of water [21]. NF also have a low thermal resistance, which limits their use in high-temperature processing, such as those used with thermoset polymers [22, 23]. This weak interfacial bonding between bamboo fibres and hydrophobic polymers leads researchers to try to overhaul natural fiber reinforced polymers by different interfacial treatments [24]. These treatments can be physical [25], chemical (such as silane [26] and alkali treatments [22]) or physicochemical such as plasma chemical vapor deposition [27]. Still, most of these treatments are not able to completely fix NF weaknesses [5].

Coatings are another way to improve the interface. Different studies have already been conducted on the coating of fibers for FRP applications, using different approaches: for example, flax fibers have been grafted with a homogenous TiO_2, 100 nm-thick film using a Sol–Gel technique resulting in more hydrophobic fibers and better mechanical properties of the composites [28].

Organic coatings, such as polymeric coatings, have also been studied to enhance properties of natural and synthetic fibers. The Addition of nanoparticles such as carbon nanotubes [29] or silica fume [30] in a fiber coating leads to a significant enhancement of the inter-laminar and ultimate tensile strength (UTS) of composites. These particles increase the toughness at the interface, stopping the crack propagation [31].

A nano-reinforced coating would be appropriate for bamboo due to its high concentration of flaws and irregularity along the fiber. The coating would heal the surface of the fiber while nanoparticles would fill flaws and holes [32]. Furthermore, according to previous studies, it would significantly improve interfacial properties and mechanical properties.

Nano-reinforcement with inorganic nanoparticles such as spherical silica fume (SiO_2 amorphous nanoparticle) are well known and studied and should be appropriate for bamboo. However, the use of innovating natural nanoparticles, such as cellulosic nanoparticles, would be an even more suitable solution to create a fully bio-based composite [33]. Starch nanocrystals (StN) are very interesting bio-sourced nanoparticles obtained from raw starch extracted from staple foods, such as potatoes, wheat, and corn. During the last decade, StN became a good alternative as nano-reinforcement because of their low cost and simple synthetis process [34].

Unfortunately, non-functionalized StN are highly hydrophilic and their mechanical properties are lower than those of synthetic nanoparticles [35, 36]. However, a proper treatment combined with a good dispersion would make them excellent for improving interfacial properties of BF.

This study focuses on the development of a fully bio-based composite material made of BF and bio-epoxy matrix with an improved interface.

Bio-based epoxy polymer was used as a replacement of conventional Epoxy (EP), which is one of the main thermoset resins used in FRP composite manufacturing [37]. A bio-based epoxy polymer has the same structure as standard epoxys where its only difference is its renewable, bio-based source [38].

BF bundles have been coated with bio-based epoxy, silica fume-reinforced epoxy, and StN-reinforced epoxy. Then, the tensile properties of uncoated and coated fibers were determined and related to contact angle measurements. Finally, flexural properties were determined on the BF reinforced bioepoxy composites to investigate the interfacial properties.

EXPERIMENTAL WORK

Materials

BF bundles with an average diameter of 250 ± 100 μm were supplied by Sunstrand, United States. The fibers have been previously dewaxed and dried by the supplier. This is performed to remove undesired organic compound from the surface of fiber.

Fibers diameters are determined by optical microscopy and ImageJ software. Figure 1 shows a micrograph of the untreated fiber. The standard deviation of the measured cross-section along the whole length of the fiber is below 10%. In addition atomic force microscopy (AFM) was used to determine the average roughness of the fiber's surface. Untreated BF bundles have a roughness of 0.17 ± 0.02 μm (Fig. 2). Only fibers with similar average diameters and roughness have been selected for the characterization of the effect of different coatings and the composites processing.

The bio-based epoxy resin and fast hardener were supplied by SuperSap. Silanized silica fume with an average

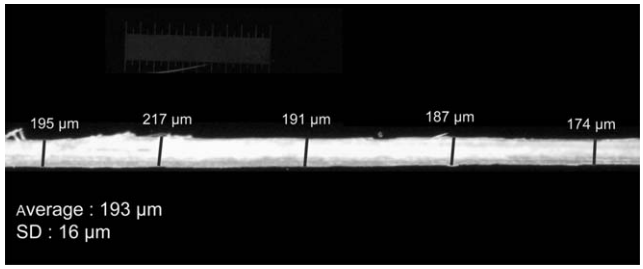

FIG. 1. Optical microscopy of an untreated BF bundles.

 DOI 10.1002/pc

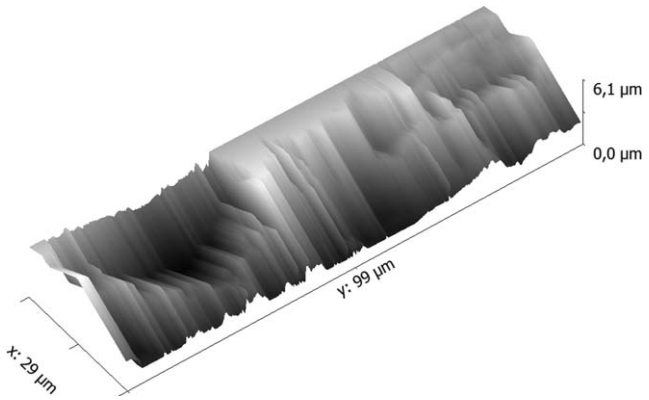

FIG. 2. AFM 3D surface representation of an untreated BF bundles.

diameter of 100 ± 50 nm was provided by Cabot. Spherical starch nanoparticles with an average diameter of 200 ± 50 nm were synthesized from raw starch according to Tehfe methodology [39]. The fibers are listed in Table 2.

Coating of the BF

Five weight percent of nanoparticles were dispersed in the bio-based epoxy resin using a high shear mechanical mixer at 1,500 rpm during 30 min. Once homogenous, the bio-epoxy/nanoparticles mixture was diluted in a large volume of acetone (1:50 weight ratio).

Addition of SiO_2 or StN to bio-based epoxy significantly increases the viscosity of the system. To characterize this phenomenon, viscosity measurements were performed on both bio-based epoxy and bio-based epoxy containing nanoparticles (SiO_2 or StN) with a Brookfield viscometer equipped with a 04 spindle at 30 rpm. The viscosity of neat bio-epoxy and nano-reinforced bio-epoxy is 2,200 cPs and 8,500 cPs, respectively.

BF bundles were then dip-coated in the solution for 30 s and acetone was evaporated at room temperature, leading to the formation of a thin film on the fiber surface (Fig. 3). Fibers were weighed before and after being coated to measure the coating content. Measurements have shown that fibers are coated with approximately 10 wt% polymer. The presence of nanoparticles does not affect this content.

Composite Processing

Composites were molded with the same bio-based epoxy and 50 phr of hardener. The samples were cast at room temperature in a 110 × 12 × 3 mm Teflon mold.

TABLE 2. Material identification.

Name	Description
Raw-BF	As-received bamboo fiber
BF-Ep	Epoxy coated bamboo fiber
BF-StN	Starch nanocrystal/epoxy coated bamboo fiber
BF-SiO_2	Silanized silica fume/epoxy coated bamboo fiber

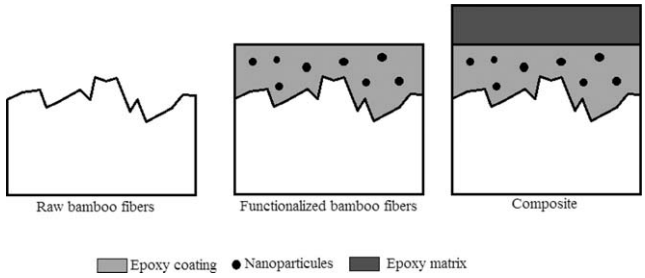

FIG. 3. Schematic illustration of the coating.

Selected fibers were weighed and aligned in the mold before pouring the resin. The samples contained approximately 25% fiber by volume.

Thermogravimetric analyses (TGA) have been performed on 15 to 20 mg samples of raw BF, fully cured epoxy matrix and composite. Thermograms are shown on Fig. 4. Both bamboo and epoxy show degradation from 100 to 550°C.

The glass transition temperature and the residual enthalpy of polymerization were determined by Differential Scanning Calorimetry (DSC) using a TA Instruments DSC Q2000 calorimeter at a rate of 10°C/min.

The T_g of the four samples is equal to 57 ± 1°C and the samples fully cured. Figure 5 shows thermogram of composites made from raw and SiO2-coated BF, showing the constant value of the T_g. Each molded composites have, therefore, the same amount of crosslinks, which should not affect the mechanical properties. Consequently, any increases would be related to the reinforcement.

Wettability Test

The wetting angle of fibers in distilled water was obtained by a Dynamic Contact Angle Tensiometer (DCA-100F). Contact angle can be calculated from Young *Eq. 1*, where γ_{sv}, γ_{sl}, and γ_{lv} are the interfacial tensions and θ_Y the Young contact angle.

$$\gamma_{SV} = \gamma_{SL} + \gamma_{LV} \times \cos\theta_Y \quad (1)$$

From *Eq. 1*, the DCA (wetting and receding angle) can be measured and calculated with *Eq. 2* where γ_l is the

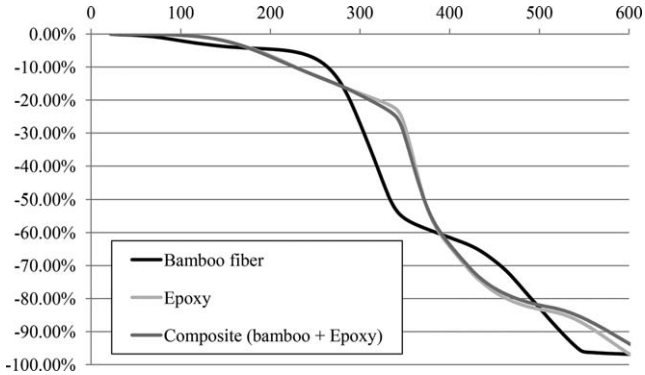

FIG. 4. TGA thermograms of BF, neat epoxy resin, and composite.

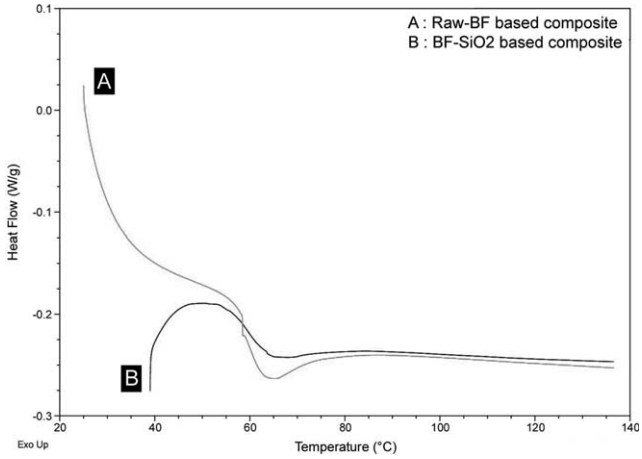

FIG. 5. DSC thermograms of (a) Raw-BF based composite and (b) BF-SiO2 based.

surface tension of the liquid and P the perimeter of the fiber.

$$\text{Wetting force} = \gamma_l \times P \times \cos\theta \quad (2)$$

The fiber diameter was calculated by taking the average of several measurements along the fiber. Fiber was inserted into the spring loaded immersion clip. A 5 mm immersion/extraction depth was selected and the test was conducted at a speed of 0.1 mm/s. An average surface tension of 72.3 mN/m at 21°C was considered for distilled water. More than 10 samples of each composition were tested.

Tensile Properties of Fibers and Composites

Tensile tests were carried out according to ASTM D2343 standard to determine the Young's modulus (E) and UTS of fibers. Originally used to study glass fibers, this standard was modified to characterize BF bundles using shorter gage length, slower speed of the testing and by testing significantly more specimens than the requirements. All the tensile tests were performed using a Zwick/Roell z050 testing machine equipped with a 100 N load cell. Tensile tests were conducted in displacement control with a crosshead speed of 1 mm/min. More than forty samples of each composition were tested.

Tensile tests were also carried out on composite according to ASTM D3039 standard. Fibers were oriented toward the loading direction. All the tests were performed using the same testing machine equipped with a 30 kN load cell and 8,404 clamps. Tensile tests were conducted in displacement control with a crosshead speed of 0.5 mm/min. More than five samples of each composition were tested.

Flexural Properties of Composites

Flexural tests were carried out according to ASTM D790 standard to determine the flexural modulus (E_f) and the flexural strength (σ_f). The span-to-thickness ratio was set at 16:1. All the flexural tests were conducted on Zwick/Roell z050 testing machine equipped with a 30 kN load cell. The crosshead speed was 1 mm/min. More than five samples for each composition were used for testing.

Scanning Electron Microscope

To study the microstructure of the fibers, scanning electron microscope (SEM) analyses were performed using a Hitachi S-3000N with the back scattering mode at 10 kV. The adhesion of the fiber to the resin was also investigated by analyzing ruptured samples. All specimens were sputtered with a thin layer of gold–platinum before analysis. Energy-dispersive X-ray spectroscopy (EDS) was coupled to SEM for element mapping. This technique was used to characterize SiO_2 scattering at the interface.

RESULTS AND DISCUSSION

Microstructural Analysis of Fibers

Microstructural analyses were conducted on raw and coated fibers. Figure 6 shows the fiber surface through the longitudinal axis before and after treatments: (a) Raw-BF; (b) BF-Ep; (c) BF-StN; (d) BF-SiO_2.

Flaws and voids are visible on the surface of raw fibers (Micrograph 6-a). These defects are partially filled with the epoxy layer (Micrograph 6-b). When SiO_2 and StN are added to the epoxy, the surface coating becomes more uniform and thicker than with neat epoxy (Micrographs 6-c and 6-d). The viscosity and density of the epoxy significantly increase with the addition of nanoparticles leading to a decrease of the diffusion of the epoxy inside the lumens of the fibers.

Cross-sectional micrographs of Raw-BF, BF-Ep, and BF-SiO_2 have been performed. Figure 7a depicts the raw BF. At lower magnification, several fibrils are observable and seem porous. At higher magnification, many lumens are noticeable, forming pores in the fiber. Figure 7b depicts the epoxy coated BF. No holes are visible and the fiber's cross section is clean compared to the raw BF. At higher magnification, only the epoxy layer is visible as it fills the lumen. Figure 7c depicts the BF coated with a nanoreinforced coating (SiO_2). Fibrils are similar to the Fig. 7b but at higher magnification, some very small lumens are not filled with the coating. The nanoreinforced coating is too viscous to enter through micro-porosity such as lumens.

To characterize the nanoparticle dispersion in the polymer coating, SEM was performed on the SiO_2/Epoxy blend at higher magnification. Figure 8 depicts the micrograph of SiO_2 nanoparticles dispersed in epoxy and the EDS mapping, highlighting the silicon from silica fume. Micrograph shows that the silica fume has an average diameter of 70–170 nm and is well dispersed in the polymer matrix. The good dispersion is confirmed by EDS spectra.

 DOI 10.1002/pc

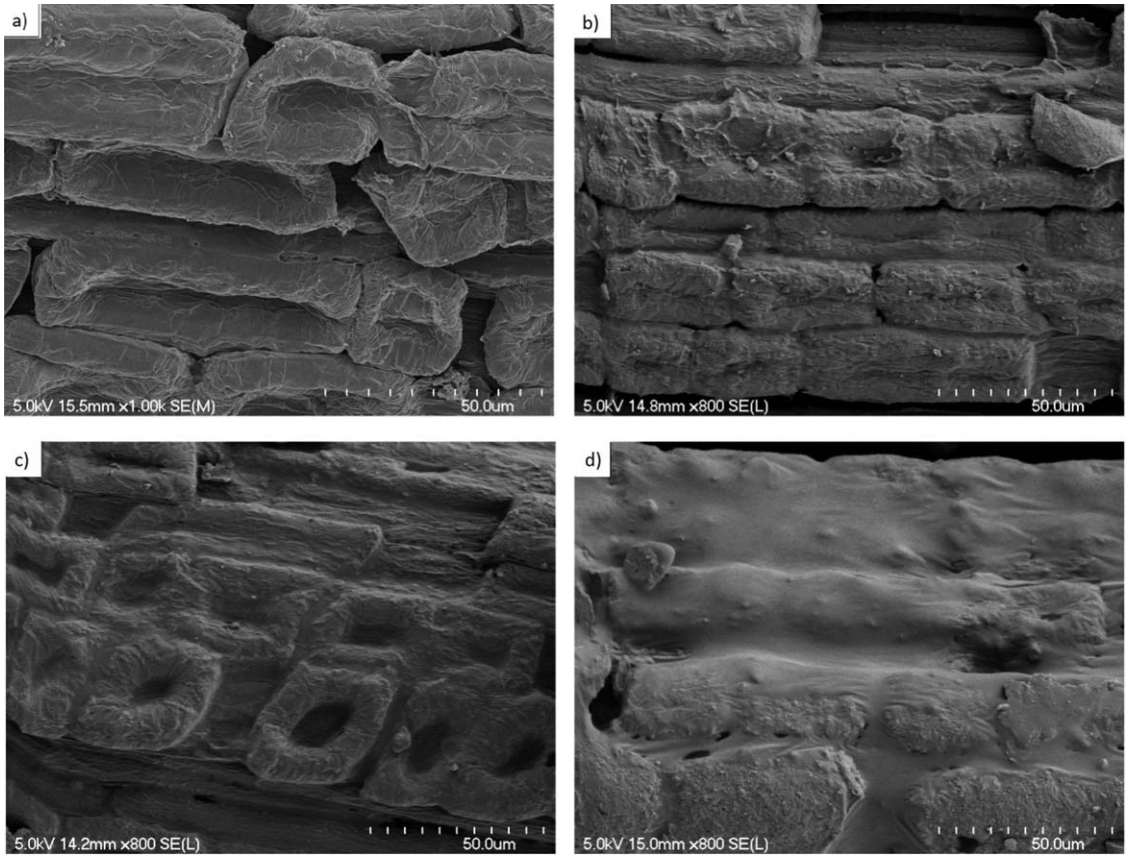

FIG. 6. SEM micrographs of BF bundles before and after coating: (a) Raw-BF; (b) BF-Ep; (c) BF-StN; (d) BF-SiO2.

The same analysis has been performed on Epoxy-StN blend. However, the chemical composition of StN is too close to the polymer to produce an appropriate contrast. So the dispersion of nanostarch could not be characterized.

Fiber Wettability

To characterize the effect of surface modification on fiber wettability, contact angles were measured (Table 3).

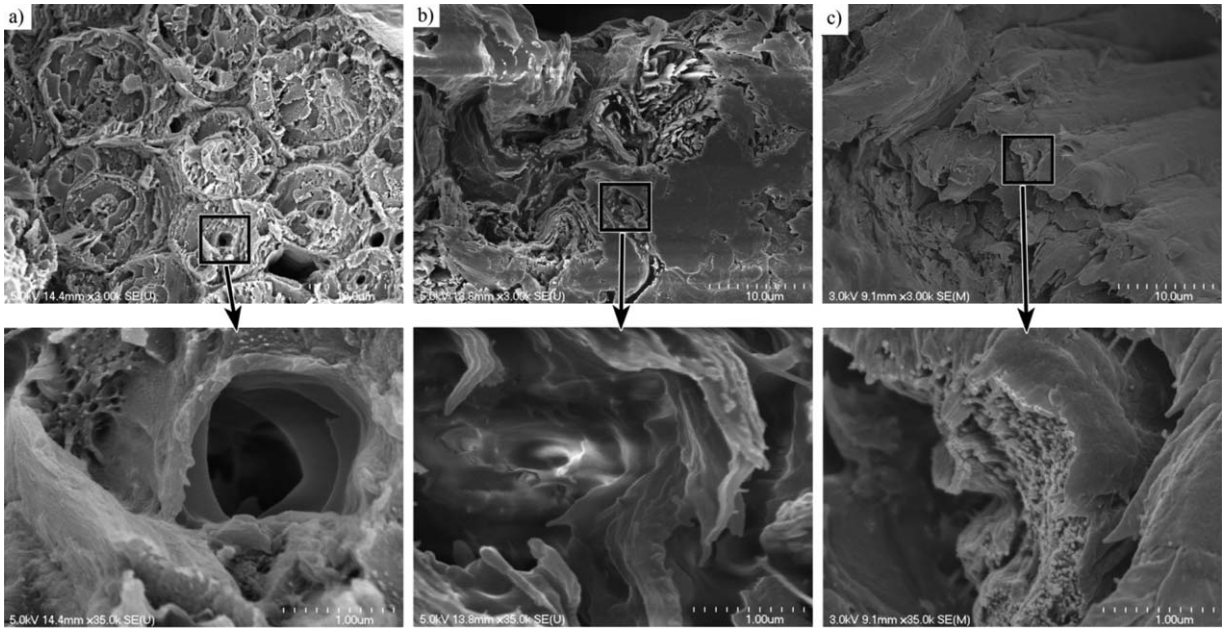

FIG. 7. Cross-section micrographs of Raw BF (8-a), BF-Ep (8-b) and BF-SiO2 (8-c) at two magnifications (×3,000 and ×35,000).

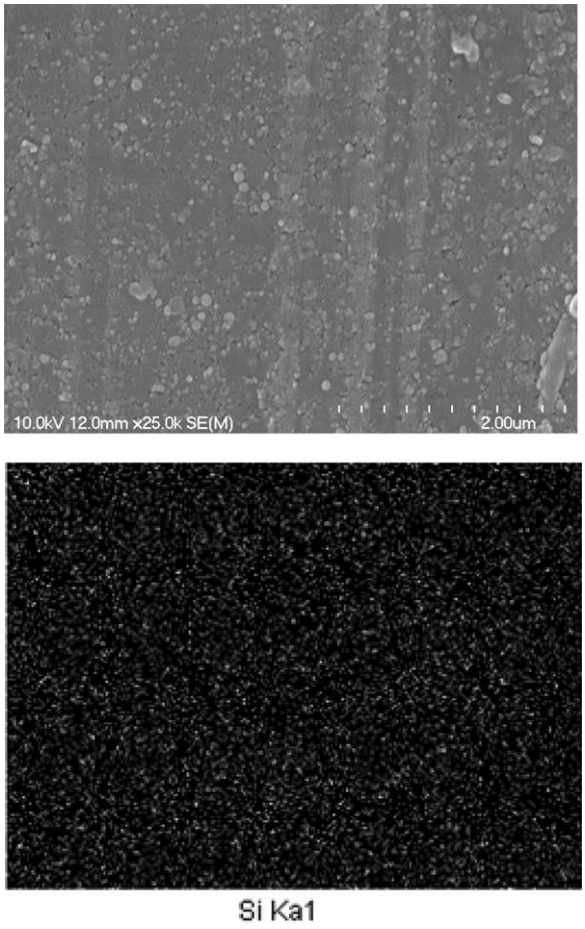

FIG. 8. SEM micrograph of SiO2 dispersed in the epoxy coating with its EDS mapping.

A wetting angle over 90° means that the surface is said to be non-wetting with that liquid. In this case, the nanoreinforced surface is hydrophobic, and the more hydrophobic the fiber is, the better the compatibility would be with a polymer matrix.

The average wetting angle of raw BF is 42°, corresponding to a hydrophilic material. When BF is coated with bio-based epoxy, the wetting angle raises to 70° as epoxy is hydrophobic.

The addition of nanoparticles (SiO_2 and StN) increases the wetting angle to 90° and 97°, respectively. Theoretically, the addition of SiO_2 and StN does not to modify the hydrophobicity of fibers, but increases the density of the coating at the fiber's surface. Microstructural characterization has highlighted that nanoreinforced coatings are well deposited at the fiber's surface. The thicker hydrophobic layer at the fiber surface explains this increase.

Mechanical Characterization of Fibers

Tensile tests were conducted on BF before and after coating. Figure 9 shows the Young's modulus (E) and the UTS of the four different samples. The Young's modulus increases by 20 to 30% independently of the type of coating. The same observation can be made for the tensile strength, which also increases after any coating of the fiber. In this case, the addition of nanoparticles could even slightly reduces the benefit brought by the neat epoxy.

TABLE 3. Measured wetting angle of untreated and coated BF.

Samples	Wetting angle (°)
Raw-BF	42 ± 13
BF-Ep	70 ± 12
BF-StN	90 ± 10
BF-SiO_2	97 ± 05

Epoxy or nanoreinforced coating should not improve mechanical properties of BF because the coating does not change the structure of the fiber. It is to be noted that the Young's moduli's and UTS' increases can be only linked to the tested BF, which is a bundle of fibers. A NF is a very complex system, constituted of micro-fibrils, containing a number of porous lumens. These lumens may be filled by the epoxy coating. When the mechanical properties of the BF are measured by tensile test, the fiber is considered to be a cylinder, which is not true because the fiber is heterogeneous and porous. By filling most of the pores with the epoxy coating, the BF's cross-section increases, allowing the fiber to sustain a higher stress. It also increases cohesion between the micro-fibrils composing the BF because the coating acts as a matrix inside the fiber which can be considered as a composite. The tested coated-BF has greater mechanical properties, even if the fiber itself still has the same structure and, therefore, the same mechanical behavior as the raw BF.

This phenomenon explains why mechanical properties slightly drop with the addition of nanoparticle in the coating: the coating may be denser at the fiber's surface but the epoxy/nanoparticle blend is too viscous to enter through small pores. Therefore, the bundle of fibrils composing the BF is more porous and the structure of the BF is closer to the raw BF. When these fibers are tested, the inaccuracy made when the cross section is measured is more pronounced because of the presence of voids inside the BF.

To confirm the hypothesis that epoxy fills the lumens in the BF, absorption tests have been performed on coated

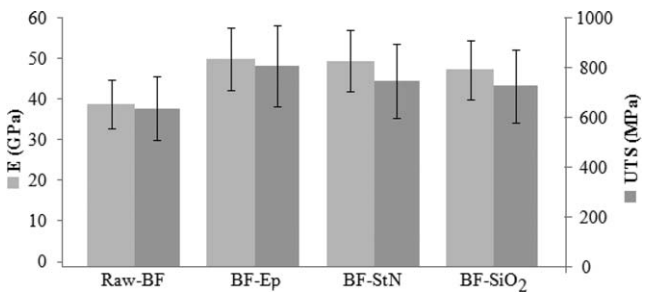

FIG. 9. Young modulus (light gray) and UTS (dark gray) of uncoated and coated BF bundles.

DOI 10.1002/pc

TABLE 4. Water absorption measurements of uncoated and epoxy-coated BF after 60 s in two medium (water or oil).

	Mass gain (%)	
	Water	Oil
Raw BF	18	13
BF-Ep	7	5

and uncoated fiber. Fibers have been immerged into water or oil for 60 s and the resulting mass gain was measured with the microbalance of the DCA. Results are presented in Table 4. Uncoated fibers absorb more than twice as much water as those that are coated. The same behavior is observed in oil meaning that even more hydrophobic fibers absorb more. The water is diffused in the BF's core by capillarity through the lumens. The epoxy fills the lumens, preventing the diffusion of liquid through the fiber and create a seal at the surface of the fiber.

Mechanical Characterization of Composites

Composites were characterized by three-point flexural and tensile tests.

As composites are manufactured by the alignment of unidirectional BF perpendicular to the beam, flexural testing tears up fibers, forcing delamination of the fibers. The reinforcement comes from the fibers meaning that the better the interface is, the better the flexural properties are. Figure 10 depicts the results for the four samples under flexion by showing the relative increase from reference.

The flexural modulus remains constant when the fiber is coated with neat epoxy, whereas it significantly increases when a thicker nano-reinforced coating is applied on the fibers (up to + 20%). A similar pattern is observed for the flexural resistance with an increase of the flexural strength of up to 24% when SiO_2 or StN are added at the interface.

Figure 10 depicts the results for the four samples under traction by showing the relative increase from reference. The same tendency is observed, namely a slight increase of the modulus, when the fiber is coated with epoxy (+ 8%), and a significant increase of the modulus is observed when the fiber is coated with epoxy containing SiO_2 or StN (+ 26%). However, there is no discernible improvement as tensile strength of all samples is really close. Reinforcement has less impact on tensile properties than on flexural properties because fibers are parallel to the testing axis, pulling out fiber rather than testing the interface.

The neat epoxy coating has a great impact on the tensile properties of the fiber but much less on the mechanical properties of the composites. The epoxy coating does not bring any advantage to the interface, except that it slightly increases the hydrophobicity of the BF. Therefore, the load transfer between the matrix and the fiber is still weak, and

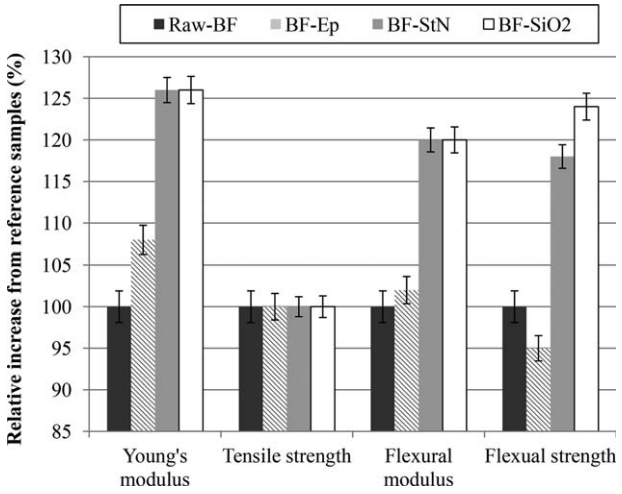

FIG. 10. Relative increases of mechanical properties of different BF based composite.

the mechanical properties of the composite do not change substantially.

Contrary to the neat epoxy coating, the nano-reinforced coatings have a significant impact on the mechanical properties of the material (up to 26% for the modulus and strength). It has to be noted that SiO_2 and StN nanoparticles provide a similar reinforcement. If most of the previous studies about nano-reinforcement were focused on conventional nanoparticles, such as SiO_2 or carbon nanotubes, StN have shown that cellulosic materials can be comparable to inorganic nanoparticles, thereby making a further step to bio-sourced composite materials.

It is well known that the interface between the two phases of a polymeric composite is generally its weakest point because the bonding between the two components limits the load transfer through the material. The interface is, therefore, the region where a stress concentration occurs

The polymer coating leads to a more hydrophobic surface of the BF. This enhances the interaction between the fiber and the epoxy matrix of the composite through Van der Waals bonds. Meanwhile, the mechanical characterization of BF-Ep specimens has shown that this mechanism has not lead to a significant increase of the properties. Conversely, the presence of nanoparticles at the interface has several effects well documented in the

TABLE 5. Composites and fibers mechanical properties.

	Tensile		Flexural	
Samples	E (MPa)	R_m (MPa)	E (MPa)	R_m (MPa)
Raw-BF	1830	88	2040	54
BF-Ep	1980	88	2077	51
BF-StN	2300	89	2455	64
BF-SiO_2	2300	88	2440	67

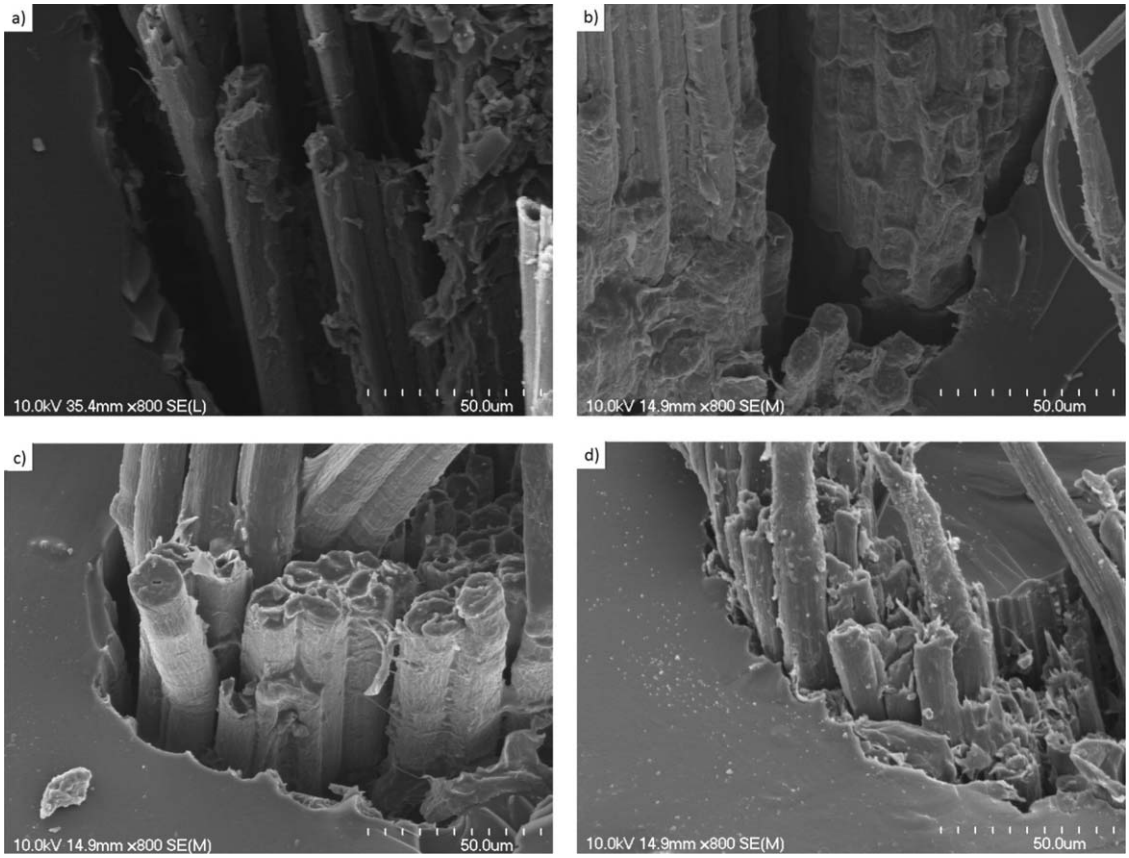

FIG. 11. SEM micrographs of the failure area after flexion of: (a) EP/Raw-BF; (b) EP/BF-Ep; (c) EP/BF-StN; (d) EP/BF-SiO2.

literature. First, the tensile and shear strength of the composite increase by the interlocking effect induced by spherical nanoparticles [40]. Then, the toughness at the interface is enhanced because the crack propagation is stopped when it faces a nanoparticle [41]. The energy of propagation is dissipated by the delamination of the nanoparticle, restraining the fiber's delamination [42]. These phenomenon have been depicted in the literature, both for nanocomposite [43] and FRP [31]. Therefore, it can be assumed that the role of the polymer coating is to sequester nanoparticles at the fibers' surface.

Finally, reinforcement with nanoparticles providing a stiffer and tougher interface that improves the ability of the material to sustain higher loads.

Table 5 sums up numerical value of both flexural and tensile properties of the composites.

Microstructural Analysis of Composites after Failure

SEM observations have been performed on the fractured areas of samples to investigate the behavior of the interphase under load. Figure 11 depicts fractured samples under flexion.

Micrograph 11-a shows the ruptured surface of the composite made with the untreated BF bundles under flexion. Large free gaps are visible around the fibers, showing that the interface did not resist to the stress. This micrograph is a good example of the weak interfacial properties between BF and bio-epoxy. Fibers slip from the polymer as soon as the rupture starts. Therefore, the load transfer from the matrix to the fiber is not possible anymore, resulting in weak composite mechanical properties. A similar behavior is observed with the BF bundles coated with epoxy (Micrograph 11-b). Fibers are debonded with no brittle failure meaning that the interface is still very weak.

Micrographs 11-c and 11-d show the EP/BF-StN and EP/BF-SiO_2 composites tested under flexion, respectively. The micrographs show that the adhesion has been improved between the fibers and the matrix. The gap between the matrix and the fiber is much thinner, and several fibers have ruptured close to the surface, showing a brittle behavior without slippage. The crack propagates throughout the composite, breaking the fiber before the delamination. This phenomenon indicates that the bonding at the interface has been enhanced by the creation of a tougher interface, as a result of the nano-reinforcement.

CONCLUSIONS

In this study, BF bundles were treated with a bio-based epoxy coating containing nanoparticles (SiO_2 or StN). Tensile tests, microscopy, and wetting angle measurements were performed on fibers to study the benefit of the coating

 DOI 10.1002/pc

on mechanical and physical properties. Composites were molded with the bio-based epoxy polymer and unidirectional fibers (Raw-BF, BF-Ep, BF-StN, and BF-SiO_2). Mechanical characterization was performed on composites, and microscopy of fractured samples was performed afterwards.

Epoxy coating homogenizes the fiber's surface, healing the important amount of defects. The epoxy coats the fiber's surface and it can also fill lumens inside the BF. Nanoparticles are well dispersed in the polymer layer, avoiding stress raisers at the interface. Mechanical characterization has been performed on uncoated/coated BF bundles. Tensile strength and modulus of epoxy-coated BF and nanoreinforced epoxy-coated BF increase up to 28%. Moreover, the epoxy-coated fiber is more hydrophobic as its wetting angle increases substantially (42 to 70°). Nano-reinforcement does not improve mechanical properties of the fiber, but it increases the wetting angle up to 95°, showing that nano-reinforced coatings make the BF more hydrophobic. Composites made with raw BF have weak mechanical properties and the characterization by SEM after failure shows a weak interface. At the interface, nanoparticles greatly improve flexural and tensile properties (up to 25%). Micrographs after failure reveal a good interface with strong bonding between fibers and matrix.

Overall, nano-reinforced coating at the interface improves the BF affinity with the polymer matrix and improves the interface. Fully bio-based composites have been made from bio-based polymer (bioepoxy), NF (BF) and bio-sourced nanoparticles (StN). These all pave the way for the utilization of NF and natural nanoparticles in composite applications.

REFERENCES

1. N.L.M. Robertson, J.A. Nychka, K. Alemaskin and J.D. Wolodko, *J. Appl. Polym. Sci.*, **130**, 2 (2013).
2. E. Bodros, I. Pillin, N. Montrelay, and C. Baley, *Compos. Sci. Technol.*, **67**, 3 (2007).
3. D.N. Saheb and J.P. Jog, *Adv. Polym. Technol.*, **18**, 4 (1999).
4. P. Wambua, J. Ivens, and I. Verpoest, *Compos. Sci. Technol.*, **63**, 9 (2003).
5. D.B. Dittenber and H.V.S. GangaRao, *Compos. Part A*, **43**, 8 (2012).
6. M. García, I. Garmendia, and J. García, *J. Appl. Polym. Sci.*, **107**, 5 (2008).
7. P. van der Lugt, A.A.J.F. van den Dobbelsteen, and J.J.A. Janssen, *Construction Building Mater.*, **20**, 9 (2006).
8. S. Ramakrishna, J. Mayer, E. Wintermantel, and K.W. Leong, *Compos. Sci. Technol.*, **61**, 9 (2001).
9. G. Lebrun, A. Couture, and L. Laperrière, *Compos. Struct.*, **103**, 151 (2013).
10. Z.N. Azwa, B.F. Yousif, A.C. Manalo, and W. Karunasena, *Mater. Des.*, **47**, 424 (2013).
11. K. Liu, H. Takagi, R. Osugi, and Z. Yang, *Compos. Sci. Technol.*, **72**, 5 (2012).
12. P. Zakikhani, R. Zahari, M.T.H. Sultan, and D.L. Majid, *Mater. Des.*, **63**, 820 (2014).
13. T.Y. Lo, H.Z. Cui, and H.C. Leung, *Mater. Lett.*, **58**, 21 (2004).
14. A.O. Oyedun, T. Gebreegziabher, and C.W. Hui, *Fuel Process. Technol.*, **106**, 595 (2013).
15. B. Sharma, A. Gatóo, and M.H. Ramage, *Construction Building Mater.*, **81**, 95 (2015).
16. X. Wang, H. Ren, B. Zhang, B. Fei, and I. Burgert, *J. R. Soc. Interface*, **9**, 70 (2012).
17. X. Li, L. Tabil, and S. Panigrahi, *J. Polym. Environ.*, **15**, 1 (2007).
18. T. Huber and J. Müssig, *Compos. Interfaces*, **15**, 2 (2008).
19. A.K. Bledzki, S. Reihmane, and J. Gassan, *J. Appl. Polym. Sci.*, **59**, 8 (1996).
20. V.A. Alvarez, R.A. Ruscekaite, and A. Vazquez, *J. Compos. Mater.*, **37**, 17 (2003).
21. Y. Pan and Z. Zhong, *Mech. Mater.*, **85**, 7 (2015).
22. M.J. John and R.D. Anandjiwala, *Polym. Compos.*, **29**, 2 (2008).
23. M. Ho, H. Wang, J-H. Lee, C. Ho, K. Lau, J. Leng, D. Hui, *Compos. Part B*, **43**, 8 (2012).
24. S. Kalia, B.S. Kaith, and I. Kaur, *Polym. Eng. Sci.*, **49**, 7 (2009).
25. M.A. Masuelli, *Introduction of Fibre-Reinforced Polymers − Polymers and Composites: Concepts, Properties and Processes*, Intech, San Luis, Argentina, (2013).
26. Y. Xie, C.A.S. Hill, Z. Xiao, H. Militz, and C. Mai, *Compos. Part A*, **41**, 7 (2010).
27. S. Mukhopadhyay and R. Fangueiro, *J. Thermoplast. Compos. Mater.*, **22**, 2 (2009).
28. M. Foruzanmehr, P. Vuillaume, M. Robert, and S. Elkoun, *Mater. Des.*, **85**, 671 (2015).
29. N.A. Siddiqui, M.-L. Sham, B.Z. Tang, A. Munir, and J.-K. Kim, *Compos. Part A*, **40**, 10 (2009).
30. A.J. Kinloch, A.C. Taylor, M. Techapaitoon, W.S. Teo, S. Sprenger, *J. Mater. Sci.*, **50**, 21 (2015).
31. F. Gauvin, P. Cousin, and M. Robert, *Fibers Polym.*, **16**, 2 (2015).
32. B. Wei, S. Song, and H. Cao, *Mater. Des.*, **32**, 8 (2011).
33. M.A.S. Azizi Samir, F. Alloin, and A. Dufresne, *Biomacromolecules*, **6**, 2 (2005).
34. M.C. Condés, M.C. Añóna, A.N. Mauria, and A. Dufresne, *Food Hydrocoll.*, **47**, 146 (2015).
35. N. Lin, J. Huang, P.R. Chang, D.P. Anderson, and J. Yu, *J Nanomater.*, **2011**, 1 (2011).
36. M. Avella, J.J. De Vlieger, M.E. Errico, S. Fischer, P. Vacca, and M.G. Volpe, *Food Chem.*, **93**, 3 (2005).
37. S.H. Goodman, *6 - Epoxy Resins*. William Andrew Publishing, Westwood, NJ (1999)
38. A. Kadam, M. Pawara, O. Yemula, V. Thamkeb, and K. Kodam, *Polymer*, **72**, 82 (2015).
39. M.A. Tehfe, R. Jamois, P. Cousin, S. Elkoun, and M. Robert, *Langmuir*, **31**, 14 (2015).
40. S.A. Meguid and Y. Sun, *Mater. Des.*, **25**, 4 (2004).
41. C. Yilmaz and T. Korkmaz, *Mater. Des.*, **28**, 7 (2007).
42. J. Spanoudakis and R.J. Young, *J. Mater. Sci.*, **19**, 2 (1984).
43. M.H.G. Wichmann, K. Schulte, and H.D. Wagner, *Compos. Sci. Technol.*, **68**, 1 (2008).